International J. of Math. Sci. & Engg. Appls. (IJMSEA)
ISSN 0973-9424, Vol. 10 No. I (April, 2016), pp. 147-175

FINITE ELEMENT METHOD TO STUDY MAGNETO-THERMO-ELASTIC WAVE IN A TRANSVERSELY ISOTROPIC HOLLOW CYLINDER

PRASHANTA PAL[1] AND MRIDULA KANORIA[2]
[1,2] Department of Applied Mathematics,
University of Calcutta,
92, A.P.C. Road, Kolkata - 700009, India.
E-mail: [1] pal.prashanta@gmail.com, [2] k_mri@yahoo.com

Abstract

This paper is concerned with the problem of magneto-thermoelastic interactions in a transversely isotropic hollow cylinder in the context of the new consideration of heat conduction with fractional order generalized thermoelasticity considering three-phase-lag model (3PL), Green-Naghdi model with energy dissipation (GN-III) and classical thermo-elasticity model (CTE). The governing equations of generalized thermoelasticity of the above model are established under the influence of a magnetic field. The Laplace transform method is used to transform the equations into the space domain, where the Galerkin finite element technique has been employed to solve the resulting equations in the transformed domain. The inversion of the Laplace transformation is carried out by applying a method of Bellman et al. The numerical estimates of the thermophysical quantities (stress and temperature) are obtained for transversely isotropic material (Mg) considering weak, normal and strong conductivity and have been depicted graphically to estimate the effects of the fractional order parameter. A comparison of the results for different theories

---

Key Words : *Generalized magneto-thermoelasticity, Fractional order, Three-phase-lag model, Green-Naghdi model, Galerkin finite element technique.*
2010 AMS Subject Classification : 74F05.

© http: //www.ascent-journals.com

(3PL, GN-III and CTE) are presented and the effect of the magnetic field is also discussed. The results for the isotropic material (Cu) and that of the transversely isotropic material (Mg) have been compared.

List of Symbols

$\mathbf{q}$	Heat flux vector
τ_q	Phase-lag of the heat flux
τ_T	Phase-lag of the temperature gradient
τ_ν	Phase-lag of the thermal displacement gradient
ξ	Parameter of the Riemann-Liouville fractional integral
ν	Thermal displacement
$\mathbf{u}$	Displacement vector
ρ	Constant mass density of the medium
K_0	Coefficient connecting temperature gradient and electric current density
T_0	Uniform reference temperature
T	Small temperature increase above the reference temperature
$\mathbf{J}$	Electric current density vector
$\mathbf{B}$	Magnetic induction vector
C_e	Specific heat of the medium at constant strain
K^*	Material constant characteristic for the GN theory
$\mathbf{H}$	Total magnetic field vector at any time
$\mathbf{h}$	Perturbed magnetic field
$\mathbf{D}$	Electric displacement vector
$\mathbf{E}$	Electric field vector
$\mathbf{F}$	Body force
μ_e	Magnetic permeability of the medium
ρ_e	Electric charge density
σ	Electric conductivity of the medium
C_T	Non-dimensional finite thermal wave speed of GN theory
ϵ	Thermo-elastic coupling constant
ϵ_0	Electric permittivity
K	Thermal conductivity
C_K	Thermal diffusivity
C_{11}, C_{12}	Elastic constants
$\beta_{rr}, \beta_{\theta\theta}$	Thermal modulii

1. Introduction

The foundations of magneto-elasticity were presented by Knopoff [32] and Chadwick [8] and developed by Kaliski and Petykiewicz [29]. In the preceding references, it was assumed that the interactions between the two fields take place by means of the Lorentz

forces appearing in the equations of motion and by means of a term from Ohm's law that describes the electric field produced by the velocity of a material charge moving in a magnetic field. Increasing attention is being devoted to the electromagnetothermoelastic problem due to its many applications in diverse fields. Investigation of the dynamic problem concerning the interactions among electromagnetic field, temperature, stresses and strains in a thermoelastic solid is immensely important because of its extensive uses in the fields of geophysics, plasma physics and related topics. Especially in nuclear fields, the extremely high temperature gradients, as well as the magnetic fields originating inside nuclear reactors, influence their design and operations. Problems related to the wave propagation in thermo-elastic or magneto-thermo-elastic solids using the generalized theories [34, 21] have been studied by several authors. Among them, Paria [43] has presented some ideas about magneto-thermo-elastic plane waves. Das and Kanoria [10] have studied magneto-thermo-elastic interaction in a functionally graded isotropic unbounded medium due to the presence of periodically varying heat sources. Roychoudhuri and Chatterjee(Roy) [49] have introduced a coupled magneto-thermoelastic problem in a perfectly conducting elastic half-space with thermal relaxation. Hsieh [26] has considered modeling of new electromagnetic materials. Das and Kanoria [11] have described magneto-thermo-elastic wave propagation in an unbounded perfectly conducting elastic solid with energy dissipation. Ezzat et al. [15] have studied electromagneto-thermo-elastic plane waves, with thermal relaxation in a medium of perfect conductivity. Problems related to magneto-thermo-elasticity with thermal relaxation have been investigated by Sherief and Youssef [52], Baksi and Bera [4], Nayfeh and Nemat-Nasser [37,38] and by Ezzat and Karamany [16].

Green-Naghdi [22, 23, 24] developed three models for generalized thermoelasticity of homogeneous isotropic material which is labelled as I, II and III. When three theories are linearized, the heat transport equation of GN I is the same as the classical heat conduction theory (based on Fourier's law) whereas both GN II and III admit propagation of thermal waves at finite speeds [24]. However GN II does not sustain propagation of magneto-thermo-elastic wave undergo attenuation and dispersion [50]. An important feature of GN III theory is that it accommodates dissipation of thermal energy due to the presence of thermal damping term. In the context of a linearized version of this theory (Green and Naghdi [23, 24], a theorem on uniqueness of solutions has been

established by Chandrasekhariah [9].

The most and relevant development in thermoelasticity theory is known as three-phase-lag model which is due to Roychoudhuri [51]. According to this model $\vec{q}(P, t+\tau_q) = -[K\vec{\nabla}T(P, t+\tau_T) + K^*\vec{\nabla}\nu(P, t+\tau_\nu)]$, where $\vec{\nabla}\nu(\dot{\nu} = T)$ is the thermal displacement gradient and the quantities τ_q, τ_T and τ_ν in this three-phase-lag model are the phase lag of the heat flux, the phase lag of the temperature gradient and the phase lag of the thermal displacement gradient in which the inequality $0 \leq \tau_\nu < \tau_T < \tau_q$ is satisfied. The heat conduction based on the TPL theory in a functionally graded hollow cylinder was investigated by Akbarzadeh et al. [1]. Quintanilla and Racke [48] studied stability of solutions in three-phase-lag heat conduction. Das et al. [12] have investigated magneto-thermoelastic response in a transversely isotropic hollow cylinder under thermal shock with three-phase-lag effect. Applying the above theory of generalized thermoelasticity, several problems have been solved by Mallik and Kanoria [36], Kar and Kanoria [30, 31], Banik and Kanoria [5, 6]. Das and Kanoria [13] have studied the problem of magneto-thermo-elastic interactions in an unbounded, perfectly conducting elastic medium due to the presence of periodically varying heat sources in the context of linear theory of generalized thermo-elasticity with energy dissipation (TEWED or GN-III model), without energy dissipation (TEWOED or GN-II model) and three-phase-lag model (3P model). Babaei and Chen [3] discussed the transient coupled thermo - piezoelectric response of a functionally graded piezoelectric hollow cylinder to dynamic loadings. Akbarzadeh and Pasini [2] introduced Phase-Lag Heat Conduction in Multilayered Cellular Media with Imperfect Bonds.

The theory of fractional derivative and integral was established in the second half of nineteenth century. The most important advantage of using fractional differential equation is their non-local property. It is well known that the integer order differential operator is a local operator but the fractional order differential operator is non-local. This means that the next state of a system depends not only upon its current state but also upon all of its historical states. This is more realistic, and this is one reason why fractional calculus has become more and more popular. The first application of fractional derivatives was given by Abel [19] who applied fractional calculus in the solution of an integral equation that arises in the formulation of the tautochrone problem. The generalization of the concept of derivative and integral to a non-integer order has been

subjected to several approaches, and some various alternative definitions of fractional derivatives appeared in [20, 25]. During recent years, several interesting models have been developed by using fractional calculus to study the physical processes particularly in the area of heat conduction, diffusion, viscoelasticity, mechanics of solids, control theory, electricity, dielectrics and semiconductors through polymers to fractals, glasses, porous, and random media, porous glasses, polymer chains, and biological systems. Ezzat et al. [17] have studied fractional order theory in thermoelastic solid with three-phase lag heat transfer. Fractional order two-temperature generalized thermoelasticity with finite wave speed was investigated by Sur and Kanoria [54]. Islam and Kanoria [27] have studied the one-dimensional problem of a fractional order two-temperature thermopiezoelasticity. Sherief et al. [53] introduced a new model of thermoelasticity using fraction calculus, proved a uniqueness theorem and derived a reciprocity relation and a variational principle. Youssef [56] introduced another new model of fractional heat conduction equation, proved a uniqueness theorem and presented one-dimensional application. Pal et al. [41] investigated fractional order generalized thermoelasticity to an infinite body with a cylindrical cavity and variable material properties. Ezzat [18] established a new model of fractional heat conduction equation using the new Taylor series expansion of time-fractional order which developed by Jumarie [28]. Sur and Kanoria [55] have studied fractional order generalized thermo-visco-elastic problem of a spherical shell with three- phase-lag effect. Problems related to the fractional order heat conduction have been studied by Povstenko [45, 46, 47]. One can refer to Padlubny [44] for a survey of applications of fractional calculus.

The purpose of this work is to present magneto-thermo-elastic interaction due to the thermal shock in the context of fractional order generalized thermoelasticity with three-phase-lag model, GN-III model and CTE model considering transversely isotropic hollow cylinder. The results obtained theoretically have been computed numerically and are presented graphically for transversely isotropic material (Mg). A complete and comprehensive analysis of the results have been presented for GN-III and three-phase-lag models in presence of magnetic field (WMF) as well as in absence of magnetic field (WOMF) considering weak ($\xi = 0.5$), normal ($\xi = 1.0$) and strong ($\xi = 1.1$) conductivity of the material and also for CTE model considering weak ($\xi = 0.5$) conductivity. We have deduced the corresponding results for isotropic material (Cu) as a particular

case and presented them graphically to compare with the results obtained for transversely isotropic material (Mg) considering three-phase-lag model, GN-III model and CTE model in presence of magnetic field for weak ($\xi = 0.5$) conductivity.

2. Formulation of the Problem and Fundamental Equations

Consider a homogeneous transversely isotropic thermo-elastic hollow cylinder of inner radius a and outer radius b with perfect conductivity having initially undisturbed state at an uniform temperature T_0, under axisymmetric thermal shock load applied into its outer boundary. Let (r, θ, z) be the cylindrical polar coordinates with the z axis as the axis of the cylinder. A magnetic field of strength **H** acts in the direction of the z axis as shown in fig. 1. Because of cylindrical symmetry of the problem all the functions are assumed to be functions of r and t only.

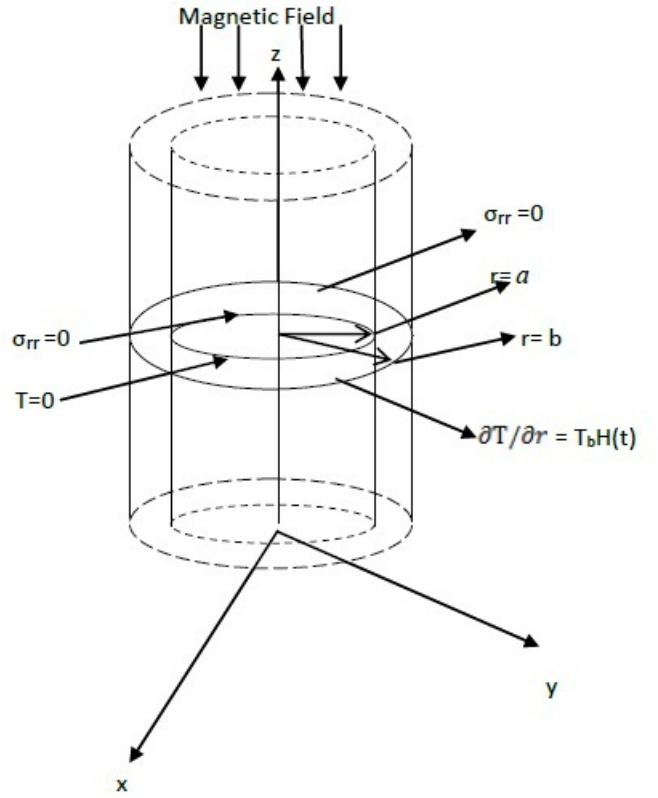


Fig.1 : Geometry of the cylinder with boundary conditions

If $\mathbf{u} = [u(r,t), 0, 0]$ be the displacement vector, then the strain vector **e** has the components $e_{rr} = \dfrac{\partial u}{\partial r},\ e_{\theta\theta} = \dfrac{u}{r},\ e_{zz} = e_{rz} = e_{r\theta} = e_{\theta z} = 0.$

The electromagnetic field is governed by Maxwell's equations (in the absence of the displacement current and charge density) (Othman [40], Nowaki [39]) as

$$\nabla \times \mathbf{H} = \mathbf{J}, \quad \nabla \times \mathbf{E} = -\frac{\partial \mathbf{B}}{\partial t}, \quad \nabla \cdot \mathbf{B} = 0, \quad \mathbf{B} = \mu_e \mathbf{H}. \tag{1}$$

The generalized Ohm's law in the deformable continua is

$$\mathbf{J} = \sigma(\mathbf{E} + \dot{\mathbf{u}} \times \mathbf{B}), \tag{2}$$

where the small effect of a temperature gradient on the conduction current $\mathbf{J}$ is neglected and $\mathbf{H} = \mathbf{H_0} + \mathbf{h}$ where $\mathbf{H_0} = (0, 0, H_0)$. The perturbed magnetic field $\mathbf{h}$ where $\mathbf{h} = (h_r, h_\theta, h_z)$ is so small that the product of $\mathbf{h}$ and $\mathbf{u}$ and their derivatives can be neglected for linearization of the field equations.

In cylindrical coordinates the equation of motion in the presence of body forces is

$$\frac{\partial \sigma_{rr}}{\partial r} + \frac{1}{r}(\sigma_{rr} - \sigma_{\theta\theta}) + (\mathbf{J} \times \mathbf{B})_r = \rho \frac{\partial^2 u}{\partial t^2}. \tag{3}$$

where the external body force is equal to Lorentz force $\mathbf{F} = (\mathbf{J} \times \mathbf{B})$.

The stress-strain-temperature relations are [33]

$$\sigma_{rr} = C_{11}\frac{\partial u}{\partial r} + C_{12}\frac{u}{r} - \beta_{rr}T, \tag{4}$$

$$\sigma_{\theta\theta} = C_{12}\frac{\partial u}{\partial r} + C_{11}\frac{u}{r} - \beta_{\theta\theta}T, \tag{5}$$

and generalized heat conduction equation for three-phase-lag model in the context of Fractional Integral is given by

$$\begin{aligned} I^{\xi-1}\left[K^* + (K + \tau_\nu K^*)\frac{\partial}{\partial t} + K\tau_T\frac{\partial^2}{\partial t^2}\right]\nabla^2 T = \left(1 + \tau_q\frac{\partial}{\partial t} + \frac{1}{2}\tau_q^2\frac{\partial^2}{\partial t^2}\right) \\ \left[\rho C_e\frac{\partial^2 T}{\partial t^2} + T_0\frac{\partial^2}{\partial t^2}\left(\beta_{rr}\frac{\partial u}{\partial r} + \beta_{\theta\theta}\frac{u}{r}\right)\right], \end{aligned} \tag{6}$$

where τ_{ij} $(i, j = r, \theta)$ are the stress tensor, T is the temperature increase over the reference temperature T_0, C_{11} and C_{12} are elastic constants, $\beta_r (= \beta_{rr})$ and $\beta_\theta (= \beta_{\theta\theta})$ are the thermal modulii, τ_T and τ_q are the phase-lag of temperature gradient and the phase-lag of heat flux respectively. Also $\nabla^2 = \frac{1}{r}\frac{\partial}{\partial r}\left(r\frac{\partial}{\partial r}\right)$ and $\tau_\nu^* = K + \tau_\nu K^*$, where τ_ν is the phase-lag of thermal displacement gradient.

The notation I^{ξ} is the Riemann-Liouville fractional integral, introduced as a natural generalization of the well-known n-fold repeated integral $I^n f(t)$ written in a convolution-type form as in Mainardi and Gorenflo [35] :

$$\begin{aligned} I^n f(t) &= \tfrac{1}{\Gamma(n)} \int_0^t (t-\tau)^{n-1} f(\tau) d\tau, \ 0 < n \leq 2, \\ &= f(t), \qquad n = 0. \end{aligned} \tag{7}$$

where $\Gamma(n)$ is the Gamma function.

In equations (3)-(6):

(i) when $\tau_T = \tau_q = \tau_\nu = 0$, then they reduce to the equations of thermo-elasticity with energy dissipation [TEWED(GN-III model)].

(ii) when $\tau_T = \tau_q = \tau_\nu = K^* = \beta_r = \beta_\theta = 0$, then they reduce to the equations of the classical theory of thermoelasticity (CTE model).

Then from Equations (1) and (2) after linearization, we get

$$\frac{\partial h_z}{\partial t} = \nu_H \left(\frac{1}{r} \frac{\partial h_z}{\partial r} + \frac{\partial^2 h_z}{\partial r^2} \right) - H_0 \frac{\partial}{\partial t} \left(\frac{u}{r} + \frac{\partial u}{\partial r} \right), \tag{8}$$

$$\frac{\partial h_\theta}{\partial t} = \nu_H \frac{\partial}{\partial r} \left(\frac{h_\theta}{r} + \frac{\partial h_\theta}{\partial r} \right), \tag{9}$$

where $\nu_H = (\sigma \mu_e)^{-1}$ is called the magnetic viscosity.

Now for a perfect electrical conductor, $\nu_H \longrightarrow 0$ as $\sigma \longrightarrow \infty$. Equation (8) leads to $h_z = -H_0 \left(\frac{u}{r} + \frac{\partial u}{\partial r} \right)$, since there is no perturbation at ∞. Then Equation (3) reduces to

$$\frac{\partial \sigma_{rr}}{\partial r} + \frac{1}{r}(\sigma_{rr} - \sigma_{\theta\theta}) + \mu_e H_0^2 \frac{\partial}{\partial r} \left(\frac{u}{r} + \frac{\partial u}{\partial r} \right) = \rho \frac{\partial^2 u}{\partial t^2}. \tag{10}$$

Using Eqs. (4) and (5), Eq. (10) becomes

$$\frac{C_{11} + \mu_e H_0^2}{\rho} \left(\frac{\partial^2 u}{\partial r^2} + \frac{1}{r} \frac{\partial u}{\partial r} - \frac{u}{r^2} \right) - \frac{\beta_r}{\rho} \frac{\partial T}{\partial r} = \frac{\partial^2 u}{\partial t^2}, \tag{11}$$

since for transversely isotropic body $\beta_r = \beta_\theta$ [14].

Introducing the following dimensionless quantities

$$U = \frac{C_{11}}{a \beta_r T_0} u, \quad (R, S) = \left(\frac{r}{a}, \frac{b}{a} \right), \quad (\sigma_R, \sigma_\theta) = \frac{1}{\beta_r T_0} (\sigma_{rr}, \sigma_{\theta\theta}), \quad \Theta = \frac{T}{T_0}, \quad \eta = \frac{Gt}{a}$$

$$(C_1, C_2) = \frac{1}{C_{11}} (C_{11}, C_{12}), \quad G^2 = \frac{C_{11}}{\rho}, \quad (\tau_q', \tau_\nu', \tau_T') = \frac{G}{a} (\tau_q, \tau_\nu, \tau_T)$$

Eqs. (4), (5), (11) and (6) become

$$\sigma_R = \frac{\partial U}{\partial R} + C_2 \frac{U}{R} - \Theta, \tag{12}$$

$$\sigma_\theta = C_2 \frac{\partial U}{\partial R} + \frac{U}{R} - \Theta, \tag{13}$$

$$R_M^2 \left(\frac{\partial^2 U}{\partial R^2} + \frac{1}{R}\frac{\partial U}{\partial R} - \frac{U}{R^2} \right) = \frac{\partial \Theta}{\partial R} + \frac{\partial^2 U}{\partial \eta^2}, \tag{14}$$

$$I^{\xi-1}\left[C_T^2 + \left(C_K^2 + \tau_\nu' C_T^2 \right) \frac{\partial}{\partial \eta} + \tau_T' C_K^2 \frac{\partial^2}{\partial \eta^2} \right] \left(\frac{\partial^2 \Theta}{\partial R^2} + \frac{1}{R}\frac{\partial \Theta}{\partial R} \right) = \left(1 + \tau_q' \frac{\partial}{\partial \eta} + \frac{1}{2}\tau_q'^2 \frac{\partial^2}{\partial \eta^2} \right) \left[\frac{\partial^2 \Theta}{\partial \eta^2} + \epsilon \frac{\partial^2}{\partial \eta^2} \left(\frac{\partial U}{\partial R} + \frac{U}{R} \right) \right], \tag{15}$$

where $R_M^2 = 1 + \dfrac{\mu_e H_0^2}{\rho G^2}$, $C_T^2 = \dfrac{K^*}{\rho C_e G^2}$, $C_K^2 = \dfrac{K}{a\rho C_e G}$ and $\epsilon = \dfrac{\beta_r^2 T_0}{\rho C_e C_{11}}$ are dimensionless constants.

The mechanical and thermal boundary conditions are given by

$$\sigma_R = 0 \quad \text{on} \quad R = 1, S \text{ (dimensionless)} \tag{16}$$

$$\Theta = 0 \quad \text{on} \quad R = 1; \quad t > 0 \tag{17}$$

$$\frac{\partial \Theta}{\partial R} = \Theta_b H(t) \quad \text{on} \ \ R = S; \quad t > 0 \tag{18}$$

The term $\Theta_b H(t)$ in Eq. (18) is heat flux applied to the outer boundary ($R = S$). Since the medium initially is at rest and undisturbed, all the state functions are assumed to be zero.

3. Method of Solution

Let

$$\left\{ \bar{U}(R,p), \bar{\Theta}(R,p) \right\} = \int_0^\infty \left\{ U(R,\eta), \Theta(R,\eta) \right\} e^{-p\eta}\, d\eta, \qquad \mathrm{Re}(p) > 0 \tag{19}$$

denote the Laplace transform of U and Θ respectively. On taking the Laplace transform equations (12)-(15) reduce to

$$\bar{\sigma}_R = \frac{d\bar{U}}{dR} + C_2 \frac{\bar{U}}{R} - \bar{\Theta}, \tag{20}$$

$$\bar{\sigma}_\theta = C_2 \frac{d\bar{U}}{dR} + \frac{\bar{U}}{R} - \bar{\Theta}, \tag{21}$$

$$R_M^2\left(\frac{d^2}{dR^2}+\frac{1}{R}\frac{d}{dR}-\frac{1}{R^2}-\frac{p^2}{R_M^2}\right)\bar{U}-\frac{d\bar{\Theta}}{dR}=0, \tag{22}$$

$$\left(\frac{d}{dR^2}+\frac{1}{R}\frac{d}{dR}-C\right)\bar{\Theta}-\epsilon C\left(\frac{d}{dR}+\frac{1}{R}\right)\bar{U}=0, \tag{23}$$

where

$$C=\frac{p^{\xi+1}\left(1+\tau_q' p+\frac{1}{2}\tau_q'^2 p^2\right)}{\left(1+\tau_\nu' p\right)C_T^2+\left(1+\tau_T' p\right)pC_K^2}. \tag{24}$$

4. Finite Element Analysis

In the finite element method, total domain is divided into a finite set of subintervals, i.e. line elements along the radial direction of the disc. The Galerkin finite element method is used to derive the stiffness and force matrices for the base element (e). For any base element (e) the displacement $\bar{U}$ and the temperature $\bar{\Theta}$ can be approximated as

$$\bar{U}=[N]^{(e)}\{U^*\}^{(e)},\quad \bar{\Theta}=[N]^{(e)}\{\Theta^*\}^{(e)}, \tag{25}$$

where $[N]^{(e)}$ is the shape function approximating the displacement and temperature fields in the base element (e). The matrices $\{U^*\}^{(e)}$ and $\{\Theta^*\}^{(e)}$ represent the nodal values of the displacement and temperature respectively. Using Eq. (25) and Galerkin finite element method over the volume of the base element $V^{(e)}$, Eqs. (22) and (23) become respectively

$$\int_{V^{(e)}}\left[R_M^2\left\{\frac{d^2}{dR^2}+\frac{1}{R}\frac{d}{dR}-\frac{1}{R^2}-\frac{p^2}{R_M^2}\right\}\bar{U}-\frac{d\bar{\Theta}}{dR}\right]N_m\,dV=0 \tag{26}$$

and

$$\int_{V^{(e)}}\left[\left\{\frac{d}{dR^2}+\frac{1}{R}\frac{d}{dR}-C\right\}\bar{\Theta}-\epsilon C\left\{\frac{d}{dR}+\frac{1}{R}\right\}\bar{U}\right]N_m\,dV=0, \tag{27}$$

where N_m is the shape function. Eqs. (26) and (27) may be reduced to the weak form. Using the local coordinates $R^*=R-R_i$, where R_i is the radius of the i th node of the base element, Eqs. (26) and (27) reduce to (dropping the asterisk for convenience)

$$\begin{aligned}\int_0^L\Bigg[-\left\{R_M^2\left(\frac{1}{R+R_i}\frac{d}{dR}-\frac{1}{(R+R_i)^2}-\frac{p^2}{R_M^2}\right)\bar{U}-\frac{d\bar{\Theta}}{dR}\right\}N_m(R+R_i)+\\ R_M^2\frac{d}{dR}\{N_m(R+R_i)\}\frac{d\bar{U}}{dR}\Bigg]dR=\left.R_M^2N_m(R+R_i)\frac{d\bar{U}}{dR}\right|_0^L\end{aligned} \tag{28}$$

and

$$\int_0^L \Bigg[-\left\{ \left(\frac{1}{R+R_i}\frac{d}{dR} - C \right) \bar{\Theta} - \epsilon C \left(\frac{d}{dR} + \frac{1}{R+R_i} \right) \bar{U} \right\} N_m(R+R_i) + \frac{d}{dR}\{N_m(R+R_i)\}\frac{d\bar{\Theta}}{dR} \Bigg] dR = N_m(R+R_i)\frac{d\bar{\Theta}}{dR}\Bigg|_0^L, \tag{29}$$

where $L = R_j - R_i$ is the length of the elements along the radial direction. The right-hand side terms of Eqs. (28) and (29) cancel each other between two adjacent elements, except the first node of the first element and the last node of the last element of the solution domain. These two nodes are located on the inner and outer boundaries of the disc. Thus applied boundary conditions may be considered as

$$\bar{\Theta} = 0, \quad \text{on} \quad R = 1 \tag{30}$$

$$b\frac{d\bar{\Theta}}{dR} = \frac{b\Theta_b}{p}, \quad \text{on} \quad R = S \tag{31}$$

$$-a\frac{d\bar{U}}{dR}\Bigg|_1 = C_2\bar{U}_1, \quad \text{on} \quad R = 1 \tag{32}$$

$$\frac{d\bar{U}}{dR}\Bigg|_M + C_2\frac{\bar{U}_M}{b} - \bar{\Theta}_M = 0, \quad \text{on} \quad R = S \tag{33}$$

where $\bar{U}_1$ and $\bar{U}_M$ are the radial displacement at the inner and outer boundaries of the disc respectively. Where 1 and M denote the first and last nodes of the solution domain respectively.

Substituting the Eq. (25) into the Eqs. (28) and (29) we obtain (dropping the asterisks for convenience)

$$\int_0^L \bar{U}_n \Bigg[R_M^2 \frac{d}{dR}\left\{N_m(R+R_i)\right\}\frac{dN_n}{dR} - R_M^2 N_m \frac{dN_n}{dR} + R_M^2 \frac{N_m N_n}{R+R_i} + p^2 N_m N_n (R+R_i) \Bigg] dR + \int_0^L \bar{\Theta}_n \left[N_m(R+R_i)\frac{dN_n}{dR} \right] dR = R_M^2 N_m(R+R_i)\frac{d\bar{U}}{dR}\Bigg|_0^L \tag{34}$$

and

$$\int_0^L \bar{U}_n \left[\epsilon C \left\{ N_m(R+R_i)\frac{dN_n}{dR} + N_m N_n \right\} \right] dR + \int_0^L \bar{\Theta}_n \left[\frac{d}{dR}\left\{ N_m(R+R_i) \right\} \frac{dN_n}{dR} - N_m \frac{dN_n}{dR} + C N_m N_n (R+R_i) \right] dR = N_m(R+R_i)\frac{d\bar{\Theta}}{dR}\Big|_0^L \tag{35}$$

Now the transfinite element Eqs. (34) and (35) are expressed in the matrix form as

$$\begin{bmatrix} (K_{11}) & (K_{12}) \\ (K_{21}) & (K_{22}) \end{bmatrix} \begin{bmatrix} \bar{U} \\ \bar{\Theta} \end{bmatrix} = \begin{bmatrix} F \\ Q \end{bmatrix}. \tag{36}$$

The submatrices (K_{11}), (K_{12}), (K_{21}), (K_{22}), F and Q are

$$K_{11}^{mn} = \int_0^L \left[R_M^2 \frac{d}{dR}\left\{ N_m(R+R_i) \right\} \frac{dN_n}{dR} - R_M^2 N_m \frac{dN_n}{dR} + R_M^2 \frac{N_m N_n}{R+R_i} + p^2 N_m N_n (R+R_i) \right] dR, \tag{37}$$

$$K_{12}^{mn} = \int_0^L \left[N_m(R+R_i)\frac{dN_n}{dR} \right] dR, \tag{38}$$

$$K_{21}^{mn} = \int_0^L \left[\epsilon C \left\{ N_m(R+R_i)\frac{dN_n}{dR} + N_m N_n \right\} \right] dR, \tag{39}$$

$$K_{22}^{mn} = \int_0^L \left[\frac{d}{dR}\left\{ N_m(R+R_i) \right\} \frac{dN_n}{dR} - N_m \frac{dN_n}{dR} + C N_m N_n (R+R_i) \right] dR, \tag{40}$$

$$F = \begin{bmatrix} 0 \\ 0 \\ . \\ . \\ 0 \\ 0 \end{bmatrix}, \quad Q = \begin{bmatrix} 0 \\ 0 \\ . \\ . \\ 0 \\ \dfrac{b\Theta_b}{p} \end{bmatrix}. \tag{41}$$

5. Numerical Results and Discussions

The solution in the space-time domain is obtained numerically by using Bellman et al. [7] method for fixed value of the space variable and for $\eta = \eta_i,\ i = 1(1)7$, where η_i's are

computed from roots of the shifted Legendre polynomial of degree 7 (see Appendix). The computations for the state variables are carried out for different values of R and values of $\eta_i = 0.0257750,\ 0.138382,\ 0.352509,\ 0.693147,\ 1.21376, 2.04612, 3.67119$. The physical data for transversely isotropic material (Mg) are taken as [14]

$$\rho = 1.74\times10^3 \text{ kg/m}^3,\ \ \epsilon = 0.0202,\ \ C_{11} = 5.974\times10^{10} \text{ N/m}^2,\ \ C_{12} = 2.624\times10^{10} \text{ N/m}^2$$

and also the physical data for the isotropic material (Copper) are taken as in [42]

$$\rho = 8.954\times10^3 \text{ kg/m}^3,\ \ \epsilon = 0.0168,\ \ \lambda = 7.76\times10^{10} \text{ N/m}^2,\ \ \mu = 3.86\times10^{10} \text{ N/m}^2$$

The material parameters are taken as $C_T = 2$ and $C_K = 1.2$.
Here in this paper we have considered three-phase-lag model. Now for this model the solution of the heat conduction law is stable if

$$\frac{2K\tau_T}{\tau_q} > \tau_\nu^* > K^*\tau_q, \tag{42}$$

where $\tau_\nu^* = K^*\tau_\nu + K$ [48]. We have assumed the values of these phase lag parameters in our paper in the way that they have satisfied the above condition. And hence for numerical calculation we have taken

$$\tau_q = 2.0\times10^{-7}\text{sec},\ \tau_T = 1.5\times10^{-7}\text{sec},\ \tau_\nu = 1.0\times10^{-7}\text{sec}.$$

The computations were carried out for $\eta = 0.14$. The results of the numerical evaluation of the thermoelastic stress and temperature are illustrated in the figures 2 to 9 for different values of R. In figures 2 to 5, these thermophysical quantities have been studied in case of three-phase-lag model (3PL model) and Green-Naghdi III model (GN-III) under the influence of magnetic field considering weak ($\xi = 0.5$), normal ($\xi = 1.0$) and strong ($\xi = 1.1$) conductivity for transversely isotropic material. Figures 6 and 7 represent the comparison of the results for different theories (3PL, GN-III and CTE) and for different types of materials (Mg and Cu) taking $\xi = 0.5$. In figures 8 and 9, the variation of the thermoelastic stress distribution are shown for different values of the magnetic field ($R_M = 1.1, 1.2, 1.3, 1.4$). Figures 10-15 represent the contour plots for radial stress (σ_R) and temperature (Θ) versus radial distance (R) and time (η) in presence of magnetic field ($R_M = 1.1$) considering weak ($\xi = 0.5$), normal ($\xi = 1.0$) and strong ($\xi = 1.1$) conductivity in the context of 3PL model.

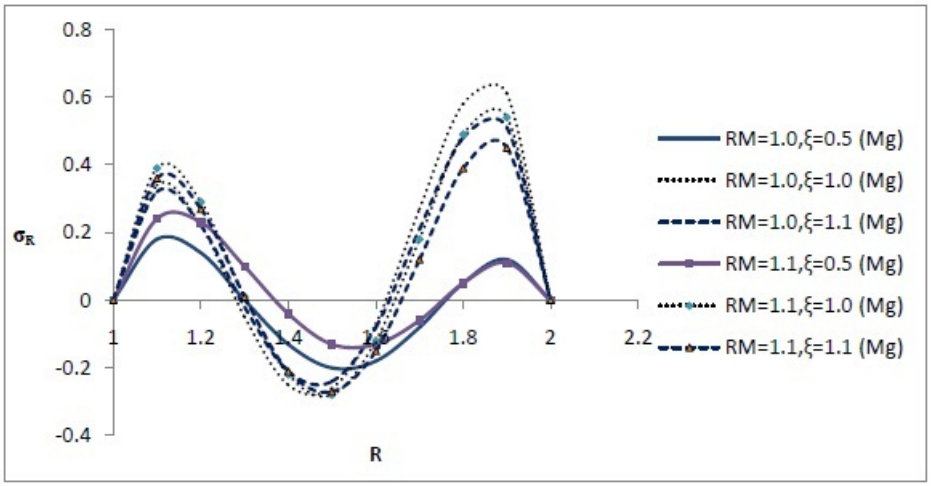


Fig. 2 Variation of radial stress σ_R against radial distance R at $\eta = 0.14$ for 3PL model.

Figure 2 represents the variation of the radial stress σ_R against radial distance R at the time $\eta = 0.14$ for 3P Lag model for weak ($\xi = 0.5$), normal ($\xi = 1.0$) and strong ($\xi = 1.1$) conductivity in the absence of magnetic field i.e. WOMF ($R_M = 1.0$) as well as in the presence of magnetic field i.e. WMF ($R_M = 1.1$) for transversely isotropic material (Mg). From this figure, it can be observed that the stress wave propagates from outer boundary to inner boundary since the heat flux is applied on the outer boundary only. The radial stress in each case is found to vanish on both the boundaries, which agrees with the imposed boundary condition. It is observed that in absence of magnetic field the radial stress σ_R is reflexive in the region $1 \leq R \leq 1.30$ and $1.76 \leq R \leq 2$ for weak conductivity ($\xi = 0.5$), in the region $1 \leq R \leq 1.28$ and $1.62 \leq R \leq 2$ for normal conductivity ($\xi = 1.0$) and in the region $1 \leq R \leq 1.29$ and $1.63 \leq R \leq 2$ for strong conductivity ($\xi = 1.1$) but in presence of magnetic field the radial stress σ_R is reflexive in the region $1 \leq R \leq 1.36$ and $1.75 \leq R \leq 2$ for weak conductivity ($\xi = 0.5$), in the region $1 \leq R \leq 1.31$ and $1.64 \leq R \leq 2$ for normal conductivity ($\xi = 1.0$) and in the region $1 \leq R \leq 1.31$ and $1.66 \leq R \leq 2$ for strong conductivity ($\xi = 1.1$). The multiple reflections of σ_R from outer to inner and from inner to outer boundary for 3P Lag model has occur due to the application of the heat flux on the outer boundary. From this figure, we can also compare the stress distribution for Mg in case of WOMF

and WMF for three-phase-lag model for different conductivities. It is noticed that the radial stress σ_R is oscillatory both for WOMF and WMF but the magnitude of σ_R is large in case of WOMF than WMF near the outer boundary for all conductivities.

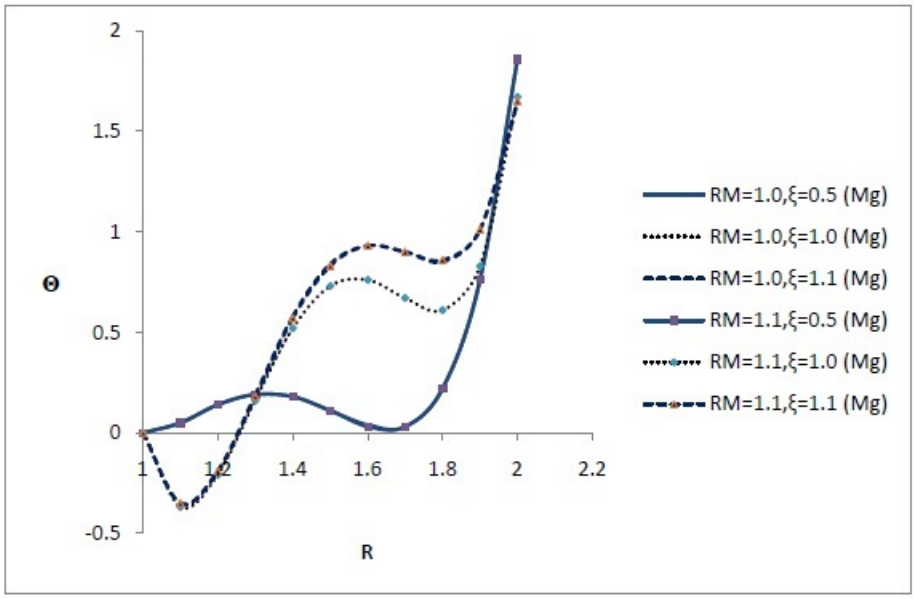


Fig. 3. Variation of temperature θ against radial distance R at $\eta = 0.14$ for 3PL model.

Figure 3 is plotted to show the variation of the temperature Θ against radial distance R at time $\eta = 0.14$ for 3P Lag model taking transversely isotropic material (Mg). It is observed that temperature (Θ) is equal to zero at the inner boundary for weak ($\xi = 0.5$), normal ($\xi = 1.0$) and strong ($\xi = 1.1$) conductivity in presence of magnetic field and also in absence of magnetic field. It is obvious, since there is no temperature on the inner boundary. Here Θ increases with the increase of radial distance and attains its maximum magnitude at the outer boundary for all the cases where the heat flux is applied. This is physically plausible. It is noticed that only for weak conductivity ($\xi = 0.5$), temperature (Θ) is positive in the whole considered region but for the other two conductivities ($\xi = 1.0$ and $\xi = 1.1$) it becomes positive only after $R = 1.21$. Now it is observed that the magnitude of the temperature (Θ) for strong ($\xi = 1.1$) conductivity is large than that of normal ($\xi = 1.0$) conductivity in the region $1.3 \leq R \leq 2$. It can also be noted that magnetic field has no effect on temperature since both the fields (magnetic and temperature) are mutually independent.

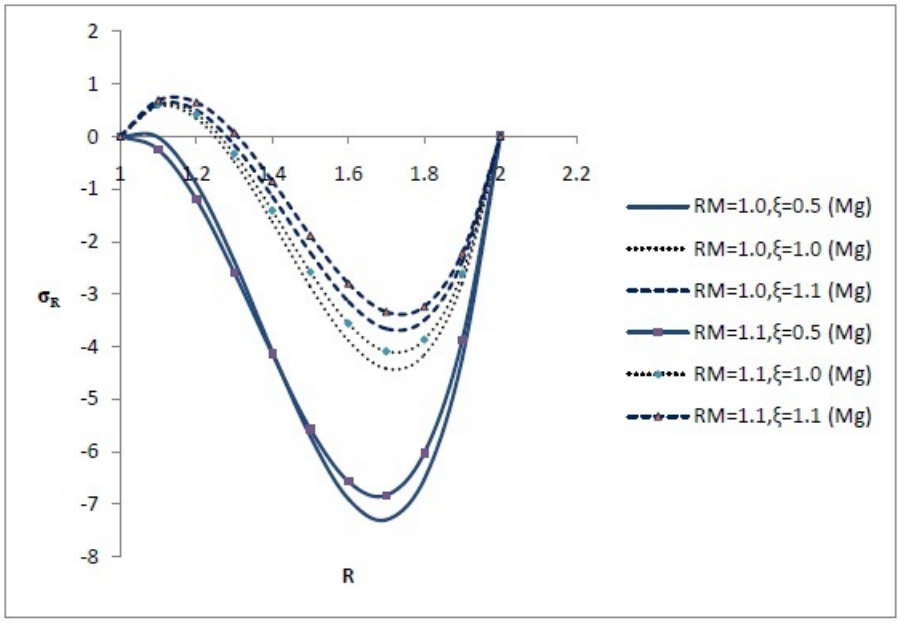


Fig. 4. Variation of temperature σ_R against radial distance R at $\eta = 0.14$ for GNIII model.

Figure 4 shows the variation of the radial stress σ_R against radial distance R at the time $\eta = 0.14$ for GN-III model taking $(\xi = 0.5, 1.0, 1.1)$ for of magnetic field i.e. WOMF $(R_M = 1.0)$ as well as in presence of magnetic field WOMF as well as WMF in case of transversely isotropic material (Mg). From this figure, it is observed that the magnitude of the radial stress σ_R is large in the case of weak $(\xi = 0.5)$ conductivity than that of normal $(\xi = 1.0)$ conductivity both for WOMF $(R_M = 1.0)$ and WMF $(R_M = 1.1)$.
Figure 5 depicts the variation of the temperature Θ against radial distance R at time $\eta = 0.14$ for GN-III model. From this figure, it is seen that at the inner boundary $R = 1$, the magnitude of the temperature Θ is 0, which agrees with the imposed boundary condition. Then the temperature Θ is gradually increases with increasing R and attains its maximum magnitude at the outer boundary $R = 2$ for all the cases where the step-input temperature is imposed. In this connection, it is to be noted that the magnitude of the temperature Θ is large for weak $(\xi = 0.5)$ conductivity than that of normal $(\xi = 1.0)$ and that is again large than that of strong $(\xi = 1.1)$ conductivity for both WOMF $(R_M = 1.0)$ and WMF $(R_M = 1.1)$.

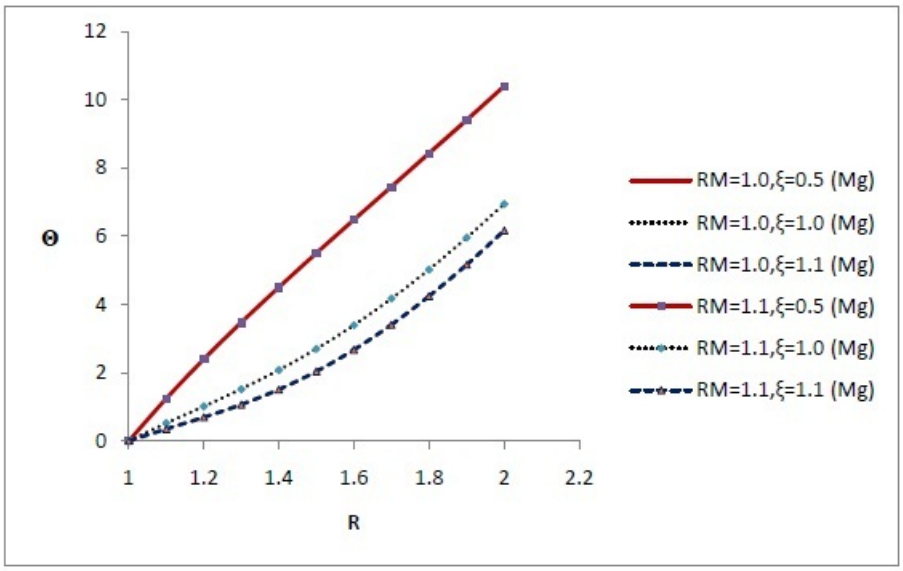


Fig. 5. Variation of temperature θ against radial distance R at $\eta = 0.14$ for GNIII model.

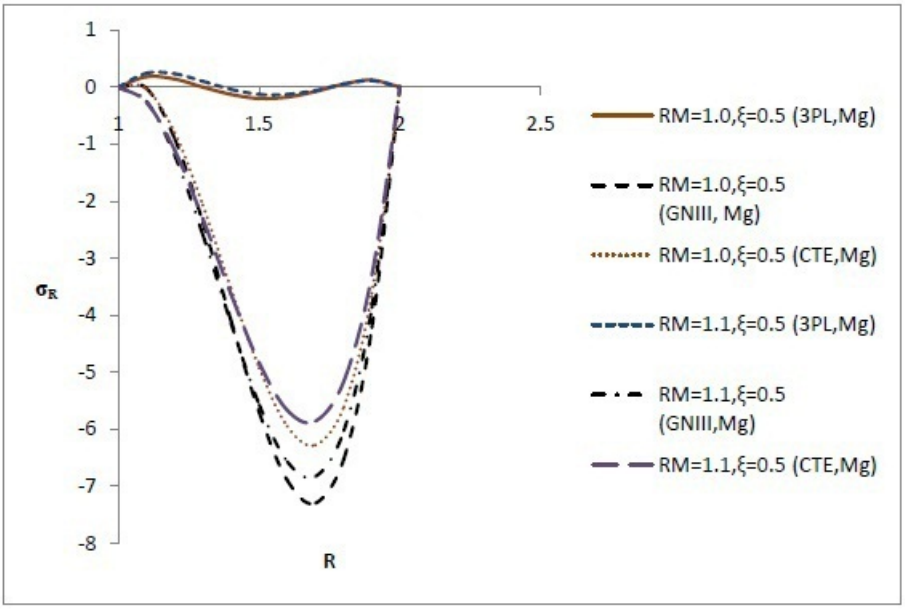


Fig. 6 : Variation of radial stress σ_R against radial distance R at $\eta = 0.14$.

Figure 6 represents the variation of the radial stress σ_R against radial distance R at the time $\eta = 0.14$ for weak ($\xi = 0.5$) conductivity. A comparison of the results obtained

for three-phase-lag model (3P Lag model), GN-III model and CTE model are analyzed in the absence of magnetic field as well as in the presence of magnetic field considering transversely isotropic material (Mg). It is observed that the magnitude of the radial stress for GN-III model is larger in comparison to CTE model, which is again larger than that of 3P Lag model for both of WOMF and WMF near the outer boundary where the heat flux is applied.

Figure 7 shows the variation of the radial stress σ_R against radial distance R at the time $\eta = 0.14$ for both the materials (Mg and Cu) in the presence of magnetic field for weak ($\xi = 0.5$) conductivity. It is noticed that the magnitude of radial stress for transversely isotropic material (Mg) is larger than that of isotropic material (Cu) for all the three thermoelasticity theories (3PL, GN-III, CTE), which is physically plausible.

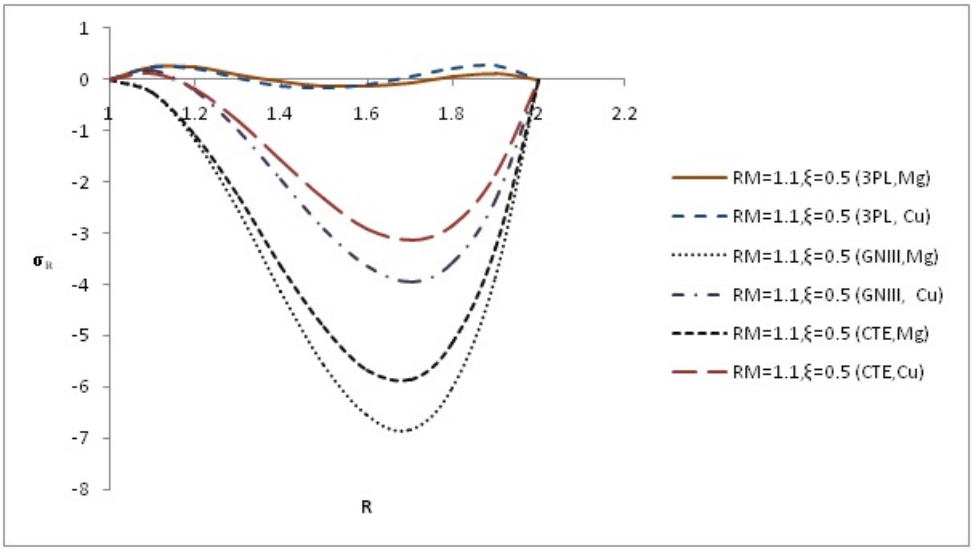


Fig. 7 : Variation of radial stress σ_R against radial distance R at $\eta = 0.14$.

Figures 8 and 9 are plotted to study the variation of radial stress σ_R versus radial distance R for normal conductivity ($\xi = 1.0$) in case of two different thermoelasticity models (3PL, GN-III) taking various values of the magnetic field $R_M = 1.1, 1.2, 1.3, 1.4$. It is seen from these figures that the magnetic field acts to decrease the magnitude of thermal stress. This is mainly due to the fact that the magnetic field corresponds to a positive force that tends to accelerate the charge carriers.

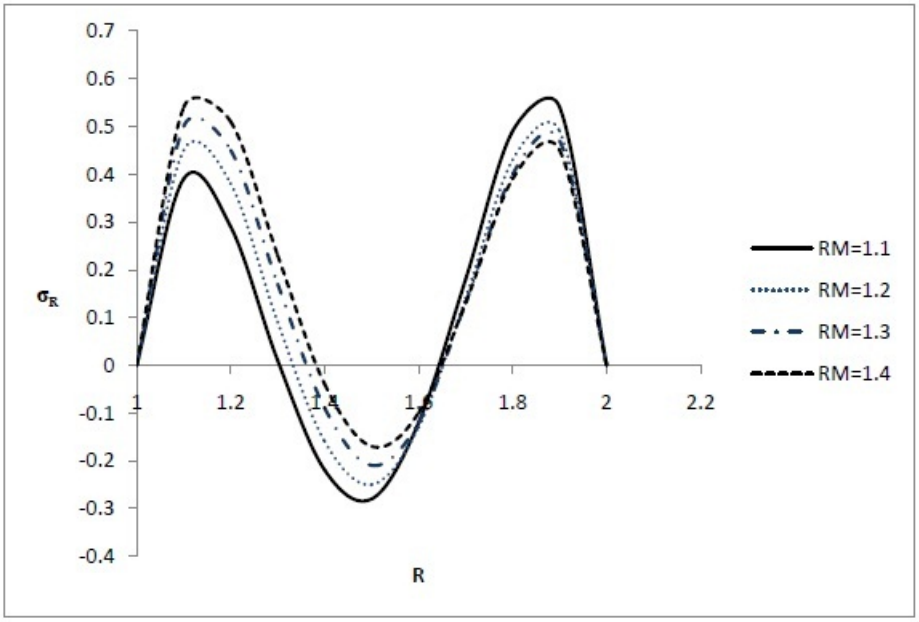


Fig. 8. Variation of radial stress σ_R against radial distance R at $\eta = 0.14$ for 3PL model

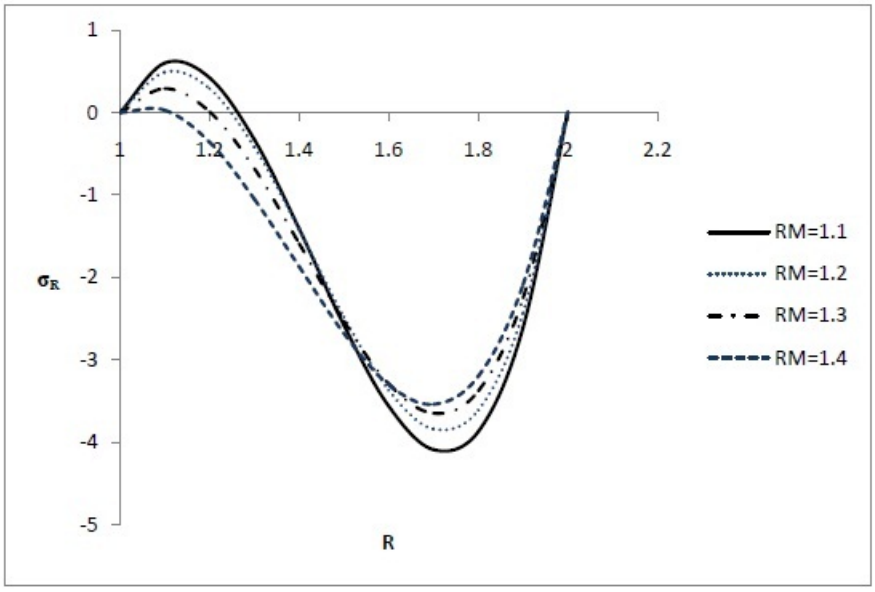


Fig. 9. Variation of radial stress σ_R against radial distance R at $\eta = 0.14$ for GNIII model

Figures 10-12 contain data on radial stress (σ_R), radial distance (R) and time (η) for weak ($\xi = 0.5$), normal ($\xi = 1.0$) and strong ($\xi = 1.1$) conductivity. Each line shows the distance and time levels for the same values of radial stress. The nature of the radial stress σ_R is oscillatory for 3PL model in all the cases of conductive material. Here the cooling effect is observed in all the contour figs. 10-12. The area of the cooling zone increases with the increment of the material conductivity ξ. Figures 13-15 consist of the data on temperature (Θ), radial distance (R) and time (η) by taking $\xi = 0.5, 1.0, 1.1$. This contours represent the distance and time levels for the same values of temperature. From the contour plots, it is observed that as the conductivity increases some negative behavior of temperature field is noticed. All the contours are drawn for 3PL model in presence of magnetic field $R_M = 1.1$ considering transversely isotropic material. These figures are very important to study the dependence of σ_R and Θ on the radial distance and time.

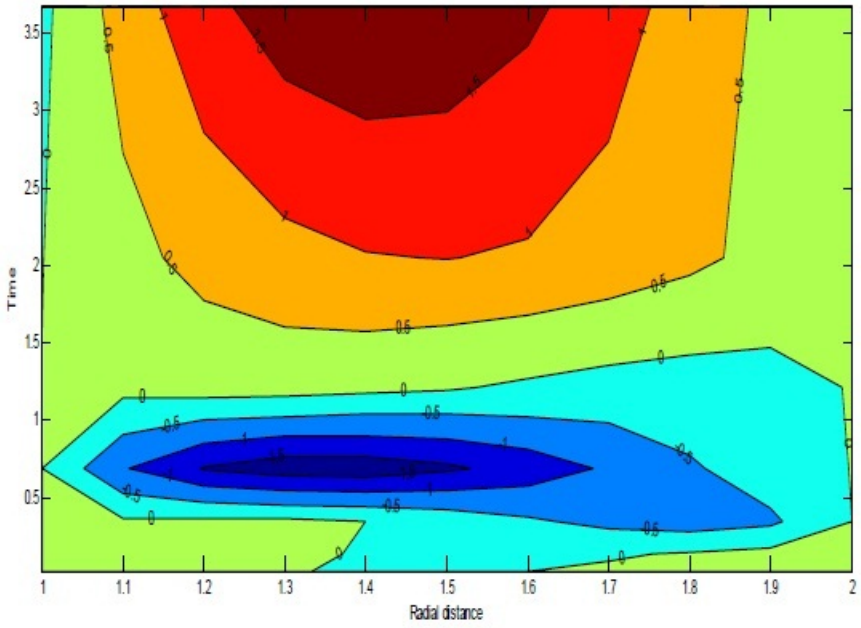


Fig. 10. Variation of radial stress σ_R against radial distance R and time η for ξ=0.5.

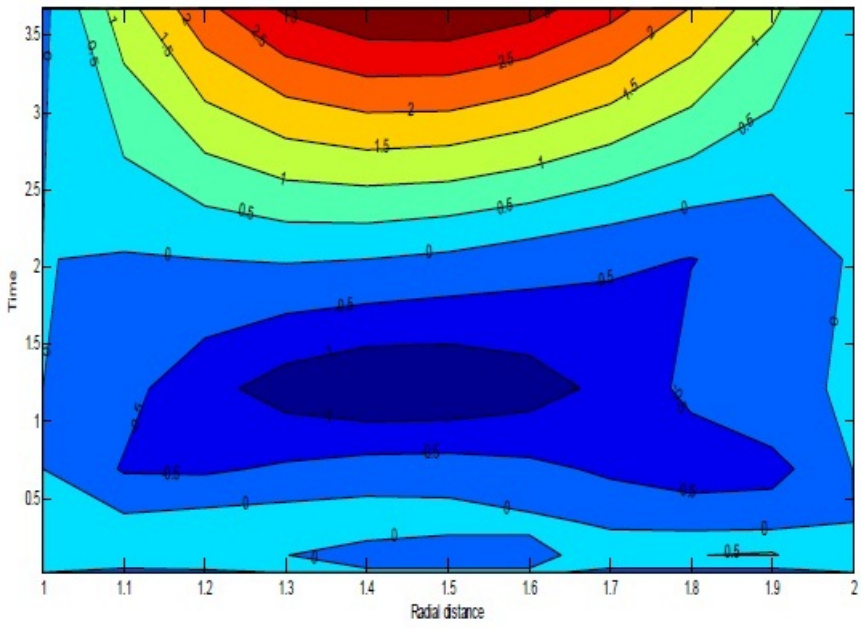


Fig. 11. Variation of radial stress σ_R against radial distance R and time η for ξ=1.0.

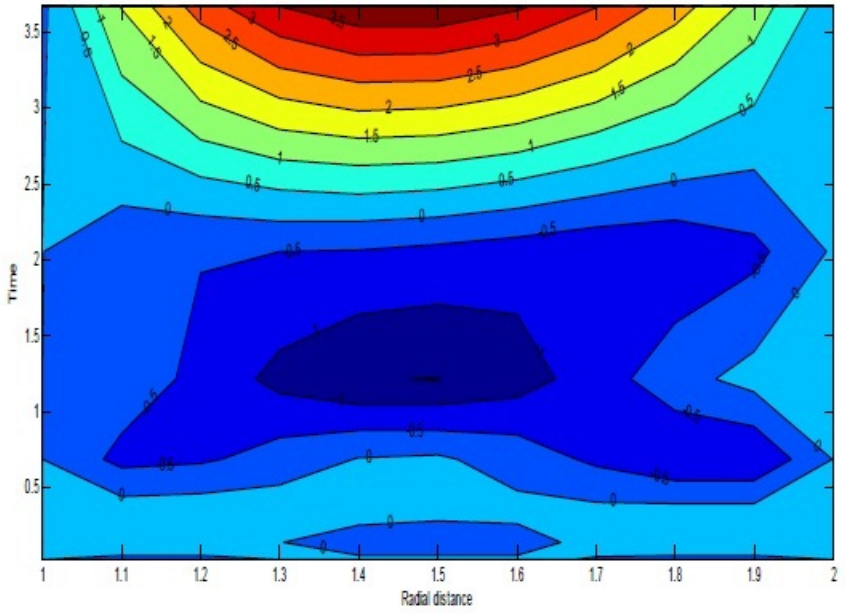


Fig. 12. Variation of radial stress σ_R against radial distance R and time η for ξ=1.1.

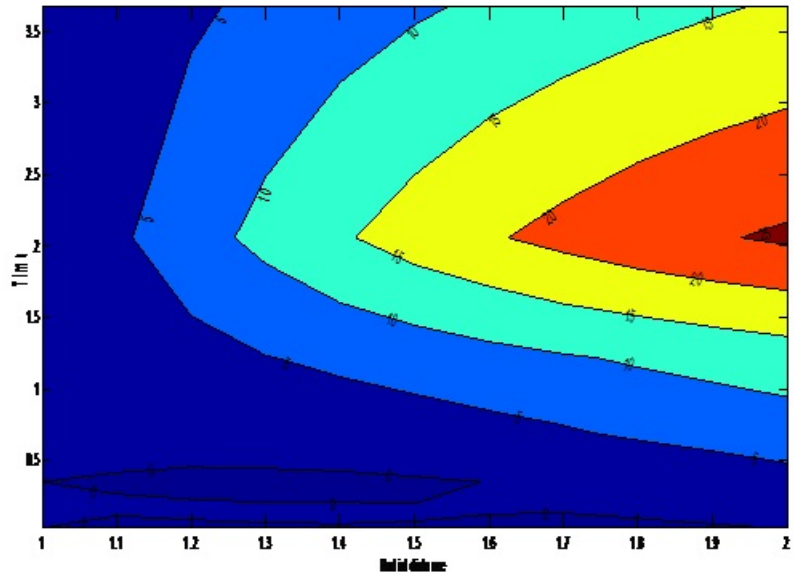


Fig. 13. Variation of temperature θ against radial distance R and time η for ξ=0.5.

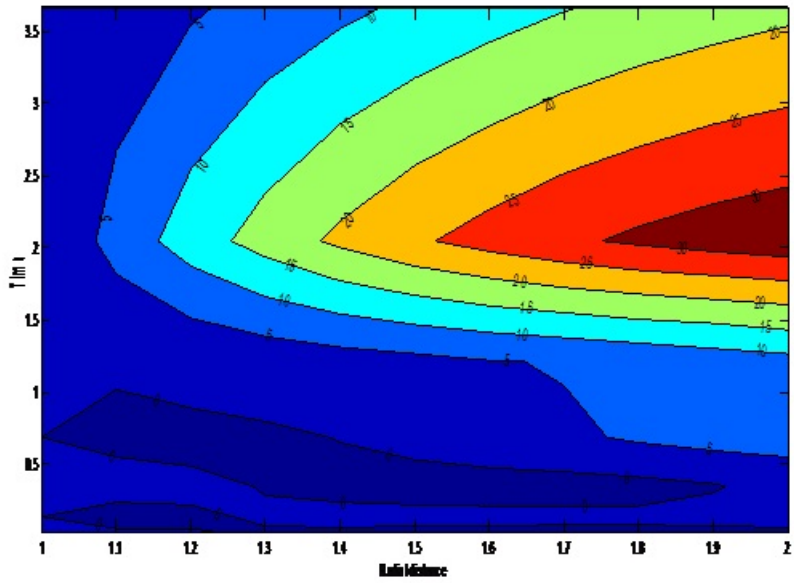


Fig. 14. Variation of temperature θ against radial distance R and time η for ξ=1.0.

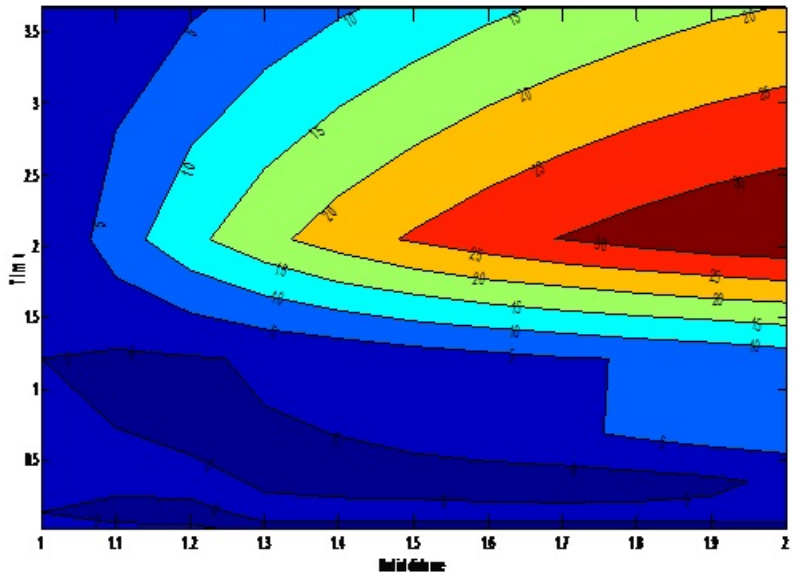


Fig. 15. Variation of temperature θ against radial distance R and time η for ξ=1.1.

Here all the results for normal conductivity ($\xi = 1.0$) agrees with that of Das et al. [12].

6. Conclusions

This paper studies the magneto-thermo-elastic stress and temperature distribution in a transversely isotropic hollow cylinder in the light of three-phase-lag model, GN-III model and CTE model in the context of fractional heat conduction equation. The method of Laplace Transform is used. Then the transformed equations are solved by Galerkin finite element technique. The numerical inversion of Laplace Transform is computed by the method of Bellman et al. The analysis of the results permit some concluding remarks:

(1) The effect of fractional order on radial stress and temperature are clearly observed in the figures.

(2) The magnetic field has an effect on radial stress but on temperature it has no such effect for three-phase-lag model, GN-III model and CTE model. Because magnetic field and temperature field are two independent field.

(3) It is obvious that there is distinct difference between three-phase-lag model, GN-III model and CTE model. The magnitude of radial stress is larger for GN-III model in comparison to CTE model which is again larger than that of 3P Lag model in presence and in absence of magnetic field.

(4) Comparison between the transversely isotropic material (Mg) and isotropic material (Cu) shows that there is a significant difference between them for three different thermoelasticity models. From the figure it is clear that magnitude of radial stress is large for transversely isotropic material (Mg) in comparison with the isotropic material (Cu).

(5) The results carried out in this paper can be used to design various fiber reinforced thermoelastic instruments under fractional order thermoelasticity theory to meet engineering requirements.

(6) This paper indicates that the generalized theory of thermoelasticity of fractional order heat transfer describes the behavior of the particles of an elastic body more realistically than the theory of generalized thermoelasticity with integer order.

(7) The result provides motivation to investigate perfectly conducting thermoelastic materials as a new class of applicable thermoelastic materials.

Acknowledgement

We are grateful to Prof. S. C. Bose of the Department of Applied Mathematics, University of Calcutta for his valuable suggestions and guidance in preparation of the paper.

Appendix

Let the Laplace transform of $\sigma_i(R,\eta)$ be given by

$$\overline{\sigma}_j(R,p) = \int_0^\infty e^{-p\eta}\sigma_j(R,\eta)d\eta. \tag{A.1}$$

We assume that $\sigma_j(R,\eta)$ is sufficiently smooth to permit the use of the approximate method we applied.

Putting $x = e^{-\eta}$ in equation $(A.1)$ we obtain

$$\overline{\sigma}_j(R,p) = \int_0^1 x^{p-1} g_j(R,x)dx, \tag{A.2}$$

where

$$g_j(R,x) = \sigma_j(R, -logx). \tag{A.3}$$

Applying the Gaussian quadrature rule to the equation $(A.2)$ we obtain the approximate relation

$$\sum_{i=1}^{n} W_i x_i^{p-1} g_j(R,x_i) = \overline{\sigma}_j(R,p), \tag{A.4}$$

where x_i's$(i = 1, 2, ...n)$ are the roots of the shifted Legendre polynomial and W_i's$(i = 1, 2, ...n)$ are the corresponding weights [7] and $p = 1(1)n$.

For $p = 1(1)n$, the equations $(A.4)$ can be written as

$$W_1 g_j(R,x_1) + W_2 g_j(R,x_2) + \cdots + W_n g_j(R,x_n) = \overline{\sigma}_j(R,1)$$

$$W_1 x_1 g_j(R,x_1) + W_2 x_2 g_j(R,x_2) + \cdots + W_n x_n g_j(R,x_n) = \overline{\sigma}_j(R,2)$$

$$\vdots$$

$$W_1 x_1^{n-1} g_j(R,x_1) + W_2 x_2^{n-1} g_j(R,x_2) + \cdots + W_n x_n^{n-1} g_j(R,x_n) = \overline{\sigma}_j(R,n)$$

Therefore

$$\begin{pmatrix} g_j(R,x_1) \\ g_j(R,x_2) \\ \vdots \\ g_j(R,x_n) \end{pmatrix} = \begin{pmatrix} W_1 & W_2 & . & . & . & W_n \\ W_1 x_1 & W_2 x_2 & . & . & . & W_n x_n \\ . & . & . & . & . & . \\ . & . & . & . & . & . \\ . & . & . & . & . & . \\ W_1 x_1^{n-1} & W_2 x_2^{n-1} & . & . & . & W_n x_n^{n-1} \end{pmatrix}^{-1} \begin{pmatrix} \overline{\sigma}_j(R,1) \\ \overline{\sigma}_j(R,2) \\ \vdots \\ \overline{\sigma}_j(R,n) \end{pmatrix}. \tag{A.5}$$

(As the matrix is the product of diag$\{W_i\}$ multiplied by Vandermonde matrix, it can be shown that the matrix is non-singular.)

Hence $g_j(R,x_1)$, $g_j(R,x_2)$, ..., $g_j(R,x_n)$ are known.

For $n = 7$ we have

Roots of the shifted Legendre Polynomial	Corresponding Weights
2.5446043828620886E-2	6.4742483084434816E-2
1.2923440720030282E-1	1.3985269574463828E-1
2.9707742431130145E-1	1.9091502525255938E-1
5.0000000000000000E-1	2.0897959183673466E-1
7.0292257568869853E-1	1.9091502525255938E-1
8.7076559279969706E-1	1.3985269574463828E-1
9.7455395617137909E-1	6.4742483084434816E-2

From equations in $(A.5)$ we can calculate the discrete values of $g_j(R, x_i)$ i,e, $\sigma_j(R, \eta_i)$; $(i = 1,2,....,7)$ and finally using interpolation we obtain the stress components $\sigma_i(R, \eta)$; $(i = R, \theta)$.

References

[1] Akbarzadeh A. H., Fu J., Chen Z., Three-phase-lag heat conduction in a functionally graded hollow cylinder. Trans Can Soc Mech Eng., 38(1) (2014), 155-171.

[2] Akbarzadeh A. H., Pasini D., Phase-lag heat conduction in multilayered cellular media with imperfect bonds. Int J Heat Mass Transf., 75 (2014), 656-667.

[3] Babaei M. H., Chen Z. T., The transient coupled thermo-piezoelectric response of a functionally graded piezoelectric hollow cylinder to dynamic loadings. Proc. R. Soc. A: Math Phys Eng Sci., 466 (2009), 1077-1091.

[4] Baksi A., Bera R. K., Eigen function method for the solution of magneto-thermoelastic problems with thermal relaxation and heat source in three dimension. Sci Direct Math comp modelling, 42 (2005), 533-552.

[5] Banik S., Kanoria M., Generalized thermoelastic interaction in a functionally graded isotropic unbounded medium due to varying heat sources with three-phase-lag effect. Math Mech solids, 18 (2013), 231-245.

[6] Banik S., Kanoria M., Effect of three-phase-lag on two-temperature generalized thermoelasticity for infinite medium with spherical cavity. Appl Math Mech., 33(4) (2012), 483-498.

[7] Bellman R., Kolaba R. E., Lockette J. A., Numerical Inversion of the Laplace Transform. American Elsevier, New York, (1966).

[8] Chadwick P., Elastic waves propagation in a magnetic field. In: Proceeding of the international congress of applied mechanics, vol. 7. Brusseles, Belgium; (1957), 143-153.

[9] Chandrasekhariah D. S., A note on the uniqueness of solution in the linear theory of thermoelasticity without energy dissipation. J. Elasticity, 43 (1996), 279-283.

[10] Das P., Kanoria M., Magneto-thermo-elastic response in a functionally graded isotropic medium under a periodically varying heat source. Int J. Thermophysics, 30 (2009), 2098-2121.

[11] Das P., Kanoria M., Magneto-thermo-elastic waves in an infinite perfectly conducting elastic solid with energy dissipation. Appl Math Mech., 30 (2009), 221-228.

[12] Das P., Kar A., Kanoria M., Analysis of magneto-thermoelastic response in a transversely isotropic hollow cylinder under thermal shock with three-phase-lag effect. J Thermal Stresses, 36 (2013), 239-258.

[13] Das P., Kanoria M. Magneto-thermo-elastic response in a perfectly conducting medium with three-phase-lag effect. Acta Mech., 223(4) (2012), 811-828.

[14] Dhaliwal R. S., Singh A., Dynamic Coupled Thermoelasticity. Hindustan Publishing Corporation, New Delhi, India: (1980).

[15] Ezzat M. A., Othman MIA, El-Karamany AS. Electro-magneto-thermo-elastic plane waves with thermal relaxation in a medium of perfect conductivity. J Thermal Stresses, 24 (2001), 411-432.

[16] Ezzat M. A., El-Karamany A. S., Fractional order heat conduction law in magneto-thermoelasticity involving two temperatures. Z Angew Math Phys., 62 (2011), 937-952.

[17] Ezzat M. A., El-Karamany A. S., Fayik MA. Fractional order theory in thermoelastic solid with three-phase lag heat transfer. Arch Appl Mech., 82 (2012), 557-572.

[18] Ezzat M. A., Magneto-thermoelasticity with thermoelectric properties and fractional derivative heat transfer. Phys B, 406 (2011), 30-35.

[19] Gorenflo R., Vessella S. Abel, Integral Equations, Lecture Notes in Mathematics. Springer: Berlin; (1991).

[20] Gorenflo R., Mainardi F., Fractional Calculus: Integral and Differential Equations of Fractional Orders, Fractals and Fractional Calculus in Continuum Mechanics. Springer Verlag, Wien and New York; (1997). 223-276.

[21] Green A. E., Lindsay K. A., Thermoelasticity. J Elasticity 2 (1972), 1-7.

[22] Green A. E., Naghdi P. M., A re-examination of the basic results of thermomechanics. Proc Roy Soc London Ser A, 432 (1992), 171-194.

[23] Green A. E., Naghdi P. M., On undamped heat waves in an elastic solid. J Thermal Stresses, 15 (1992), 252-264.

[24] Green A. E., Naghdi P. M., Thermoelasticity without energy dissipation. J Elasticity, 31 (1993), 189-208.

[25] Hilfer R., Application of Fraction Calculus in Physics. World Scientific, Singapore; (2000).

[26] Hsieh R. K. T., Mechanical modelling of new electromagnetic materials. Proc IUTAM symposium Stockholm, Sweden; (1990).

[27] Islam M., Kanoria M., One-dimensional problem of a fractional order two temperature thermopiezoelasticity. Math Mech Solid, 19(6) (2013),672-693.

[28] Jumarie G., Derivation and solutions of some fractional Black-Scholes equations in coarse-grained space and time. Application to Merton's optimal portfolio. Comput Math Appl., 59 (2010), 1142-1164.

[29] Kaliski S., Petykiewicz J., Equation of motion coupled with the field of temperature in a magnetic field involving mechanical and electrical relaxation for anisotropic bodies. Proc Vibr Probl, 4 (1960), 3-11.

[30] Kar A., Kanoria M., Analysis of thermoelastic response in a fibre reinforced thin annular disc with three-phase-lag effect. Eur J Pure Appl Math., 32 (2011), 1315-1332.

[31] Kar A., Kanoria M., Generalized thermoelastic functionally graded orthotropic hollow sphere under thermal shock with three-phase-lag effect. Eur J Mech - A/Solids, 1 (2009), 1-11.

[32] Knopoff L., The interaction between elastic wave motion and a magnetic field in electrical conductors. J Geophys Res., 60 (1955), 441-456.

[33] Lekhnitskii S. G., Theory of Elasticity of an Anisotropic Body, Mir publication, Moskow, (1980).

[34] Lord H. W., Shulman Y., A generalized dynamic theory of thermoelasticity. J Mech Phys Solids, 15 (1967), 299-309.

[35] Mainardi F., Gorenflo R., On Mittag-Lettler-type function in fractional evolution processes. J Comput Appl Math., 118 (2000), 283-299.

[36] Mallik S. H., Kanoria M., Generalized thermoviscoelastic interaction due to periodically varying heat source with three-phase-lag effect. Eur J Mech - A/Solids, 29 (2010), 695-703.

[37] Nayfeh A., Nemat-Nasser S., Thermo-elastic waves in a solids with thermal relaxation. Acta Mech., 12 (1971), 43-69.

[38] Nayfeh A., Nemat-Nasser S., Electro-magneto-thermo-elastic plane waves in solid with thermal relaxation. J Appl Mech., 39 (1972), 108-113.

[39] Nowacki W., Dynamic problem of thermoelasticity. Noordhoff International the Netherlands, 399 (1975).

[40] Othman M.I.A., Generalized Electro-Magneto-Thermoelasticity in Case of Thermal Shock Plane Waves for a Finite Conducting Half-Space with Two Relaxation Time. Mech Mech Eng., 14(1) (2010), 5-30.

[41] Pal P., Kar A., Kanoria M., Fractional order generalized thermoelasticity to an infinite body with a cylindrical cavity and variable material properties. Eur J Comput Mech., 23 (2014), 96-111.

[42] Pal P., Kar A., Kanoria M., Effect of three-phase-lag on two-temperature generalized thermoelasticity for homogeneous isotropic half space. Int J Mat Sci Eng Appl., 8 (2014), 81-104.

[43] Paria G., On magneto-thermo-elastic plane waves. Proc Camb Phil Soc., 58 (1962), :527-531.

[44] Podlubny I., Fractional Differential Equations. New York: Academic Press, (1999).

[45] Povstenko Y. Z., Fractional Catteneo-type equations and generalized thermoelasticity. J Thermal Stresses, 34 (2011), 94-114.

[46] Povstenko Y. Z., Time-fractional radial heat conduction in a cylinder and associated thermal stresses. Arch Appl Mech., 82 (2012), 345-362.

[47] Povstenko Y. Z., Fractional heat conduction in infinite one-dimensional composite medium. J Thermal Stresses, 36 (2013), 351-363.

[48] Quintanilla R., Racke R., A note on stability in three-phase-lag heat conduction. Int J Heat and Mass Transfer, 51 (2008), 24-29.

[49] Roychoudhuri S. K., Chatterjee(Roy) G., A coupled magneto-thermo-elastic problem in a perfectly conducting elastic Half- space with thermal relaxation. Int J Math and Mech Sci., 13(3) (1990), 567-578.

[50] Roychoudhuri S. K., Magneto-thermo-elastic waves in an infinite perfectly conducting solid without energy dissipation. J. Tech. Phys., 47(2) (2006), 63-72.

[51] Roychoudhuri S. K., On a thermoelastic three-phase-lag model. J Thermal Stresses, 30 (2007), 231-238.

[52] Sherief H. H., Youssef H. M., Short time solution for a problem in magneto thermoelasticity with thermal relaxation. J Thermal Stresses, 27 (2004), 537-559.

[53] Sherief H. H., El-Said A., Abd El-Latif A., Fractional order theory of thermoelasticity. Int J Solids Struct, 47 (2010), 269-275.

[54] Sur A., Kanoria M., Fractional order two-temperature thermoelasticity with finite wave speed. Acta Mech., 223 (2012), 2685-2701.

[55] Sur A., Kanoria M., Fractional order generalized thermo-visco-elastic problem of a spherical shell with three-phase-lag effect. Latin J. Solid Struct., 11 (2014), 1132-1162.

[56] Youssef H. M., Theory of fractional order generalized thermoelasticity. J. Heat Transfer (ASME), 132 (2010), 1-7.